

Supporting Information

Attapulgite as skeleton for fabrication of magnetic structural-functional materials with superhydrophobic shell

Yanbin Wang,^{a,b} Yijing Li,^{a,b} Jihai Li,^{a,b} Yujing Zhang,^c Zhiying Duan,^{a,b} Feng Zhou,^d Xin Xie,^{a,b} Qiong Su^{a,b*} and Shaofeng Pang^{a,b*}

[a]. Chemical Engineering Institute, Northwest Minzu University, Lanzhou, 730030, P. R. China

[b]. Key Laboratory of Environmental Friendly Composite Materials and Biomass in Universities of Gansu Province, Northwest Minzu University, Lanzhou, 730030, P. R. China

[c]. College of Chemistry and Chemical Engineering, Northwest Normal University, Lanzhou 730070, P. R. China

[d]. Dalian National Laboratory for Clean Energy, Dalian Institute of Chemical Physics, Chinese Academy of Sciences, 457 Zhongshan Road, Dalian 116023, P. R. China

Table of contents

I. Materials and reagents.....	S1
II. Characterization methods.....	S1
III. Schematic illustration.....	S2
IV. Partial characterization results.....	S3

I. Materials and reagents

Attapulgite (ATP) was obtained from Jiangsu Huixin Atta Co., Ltd.(Jiangsu, China). Nitrobenzene (NB) was provided by Xi long Chemical Co., Ltd.(Guangdong, China). Silane coupling agents, such as (3-mercaptopropyl) trimethoxysilane (MPTMS), methyltrimethoxysilane (MTMS) and *n*-propyltrimethoxysilane (PTMS), was purchased from Shanghai Maclean Biochemical Technology Co., Ltd., China. All other solvents and chemicals were obtained commercially and were used as received.

II. Characterization methods

The structures of as-prepared samples were observed by the field emission scanning electron microscopy (FE-SEM, Carl Zeiss-Ultra Plus, Germany). WCA (water contact angle) was measured by a POWEREACH JC2000D goniometer (Made in China). The wettability of the samples was evaluated by WCA measurement, which performed on a glass substrate using a water droplet of $\sim 5 \mu\text{L}$ using a micrometer syringe. At least five measurements were carried out to obtain each value. The error in contact angle measurements was $\pm 2^\circ$. The profiles of the contact angle were photographed using the digital camera of the goniometer. The elemental analysis was carried out with a multichannel EDS device XFlash Detector 5010 125 eV, Quantax Bruker (Germany). EDS measurements were carried out with relatively low voltage too. The Fe content of the samples were measured by using inductively coupled plasma atomic emission spectrometry (ICP-AES), by using an Iris advantage Thermo Jarrel Ash device. XRD measurements were performed by using a STADIP automated transmission diffractometer (STOE) equipped with an incident beam curved germanium monochromator with $\text{CuK}\alpha 1$ radiation. The XRD patterns were scanned in the 2θ range of $5\text{-}85^\circ$. For data interpretation, WinXpow software (STOE) and the database of powder diffraction files (PDF) of the International Centre of Diffraction Data (ICDD) were used. FT-IR spectra were registered in the $500\text{-}4000 \text{ cm}^{-1}$ region with a resolution of 1 cm^{-1} by a Nicolet 5700 spectrometer. For each FT-IR spectrum, the 0.5 mg of sample was uniformly mixed with 100 mg of potassium bromide, and then the mixture was laminated with a tablet press for further analysis. The X-ray

photoelectron spectroscopy (XPS) measurements were performed by using a VG ESCALAB 210 instrument equipped with a dual Mg/Al anode X-ray source, a hemispherical capacitor analyzer, and a 5 keV Ar⁺ ion gun. All spectra were registered by using nonmonochromatic MgK α (1253.6 eV) radiation. The samples were attached to a stainless steel sample holder by using double-sided adhesive carbon tape. The electron binding energy was referenced to the C1s peak at 284.8 eV. The peaks were fitted by Gaussian-Lorentzian curves after Shirley background subtraction. For quantitative analysis, the peak area was shared by the element-specific Scofield factor and the transmission function of the analyzer. The background pressure in the chamber was less than 10⁻⁷ Pa. The BET surface areas and pore-size distribution was calculated from the desorption isotherm by using the Barrett, Joyner, and Halenda (BJH) method (Autosorb iQ, Quantachrome, U.S.A.). Thermogravimetric analysis (TGA) was performed on a Perkin Elmer STA6000 thermogravimetric analyzer under an oxygen atmosphere at a heating rate of 10 °C min. A vibrating sample magnetometer (Lakeshore 7304) was used at room temperature to measure the magnetization. The mixtures of the adsorbent and NB solution were shaken in a thermostatic shaker water bath (SHA-BA). The shake amplitude was 20mm. In order to make the mixtures contact uniformly, the shake speed was adjusted at 140 rpm with back and forth oscillating form. The temperature was set at 25°C. Besides, all the digital pictures were taken with a Canon EOS-60D camera.

III. Schematic illustration

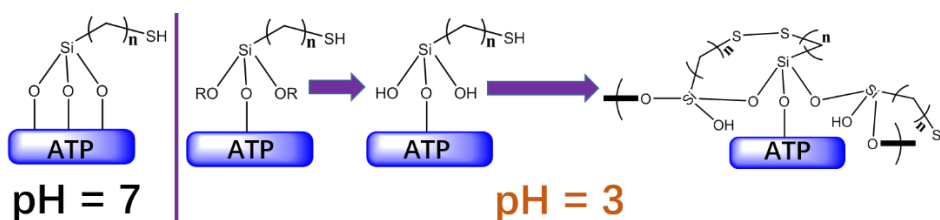
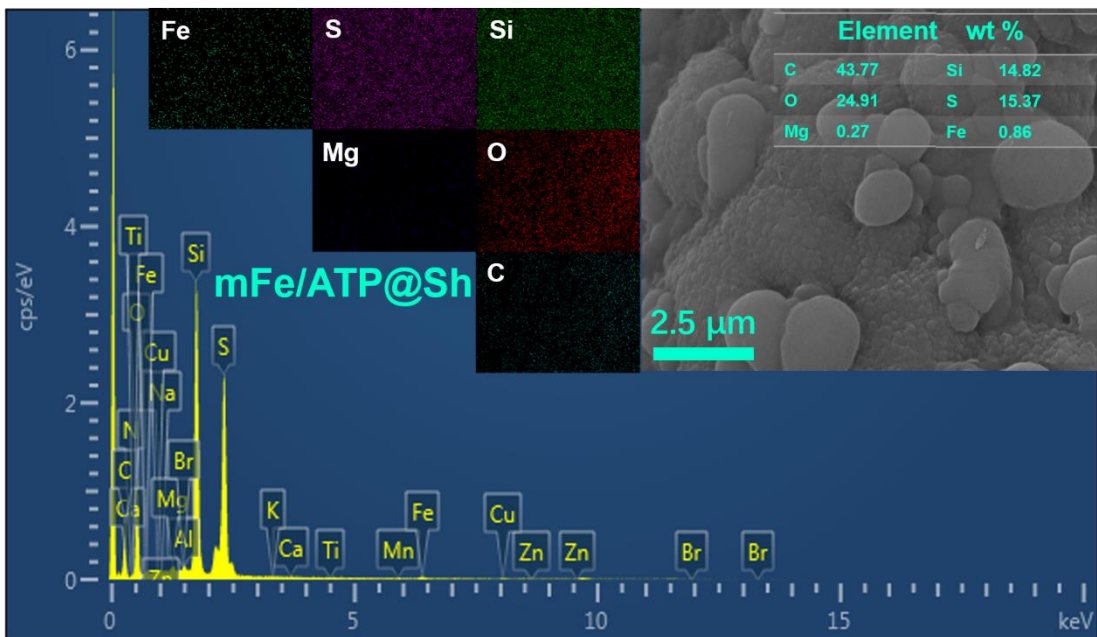
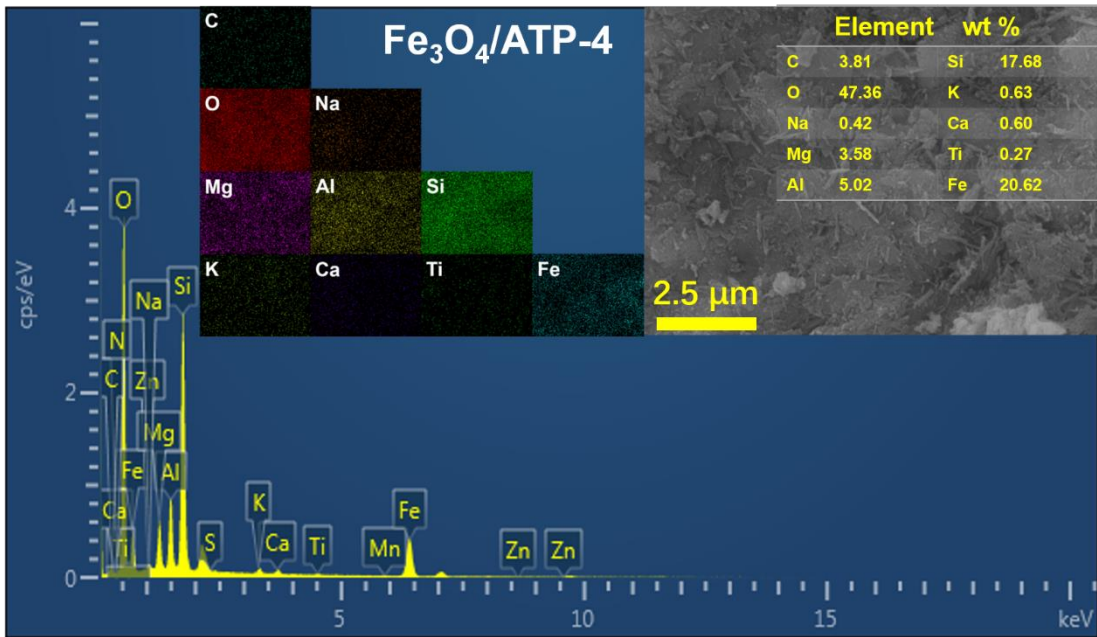


Figure S1. Schematic illustration of the possible formation process of protective shell.

IV. Partial characterization results



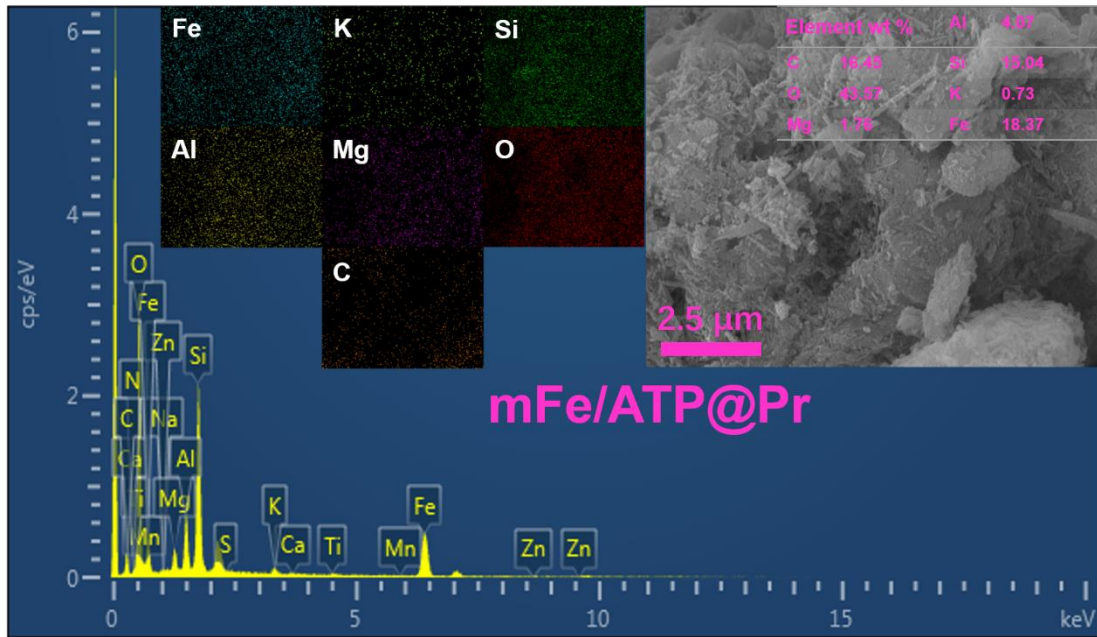


Figure S2. Detailed information on the elemental composition that was provided by electron microscopy combined with energy-dispersive X-ray spectroscopy (SEM-EDS).

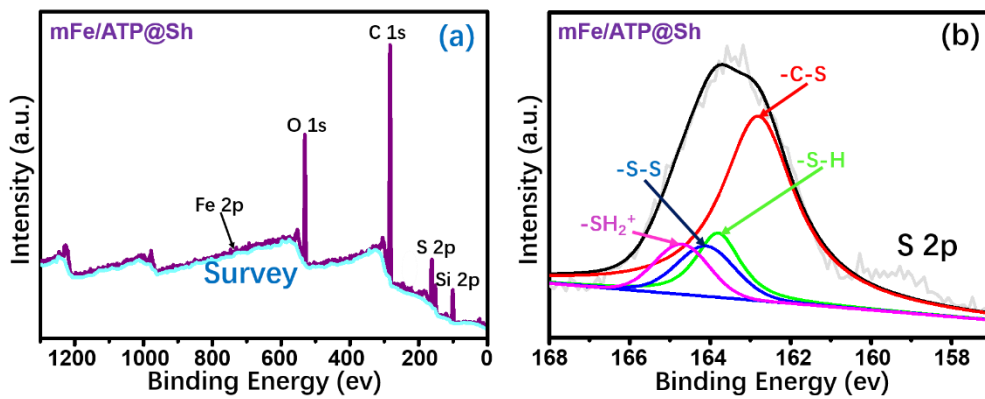


Figure S3. XPS spectra (a) and S 2p spectra (b) of mFe/ATP@Sh.

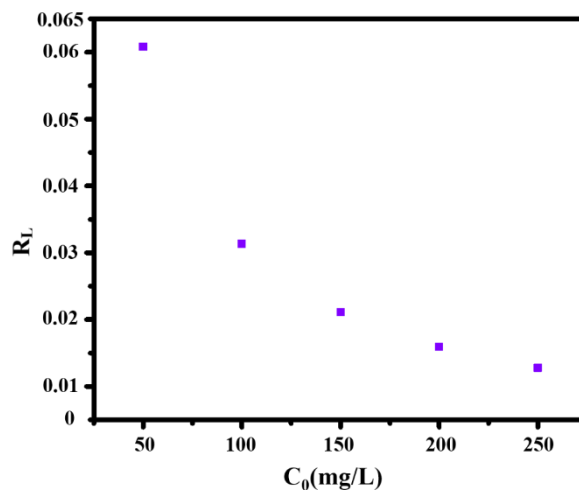


Figure S4. Plot of the R_L values for NB adsorption at different initial concentrations.

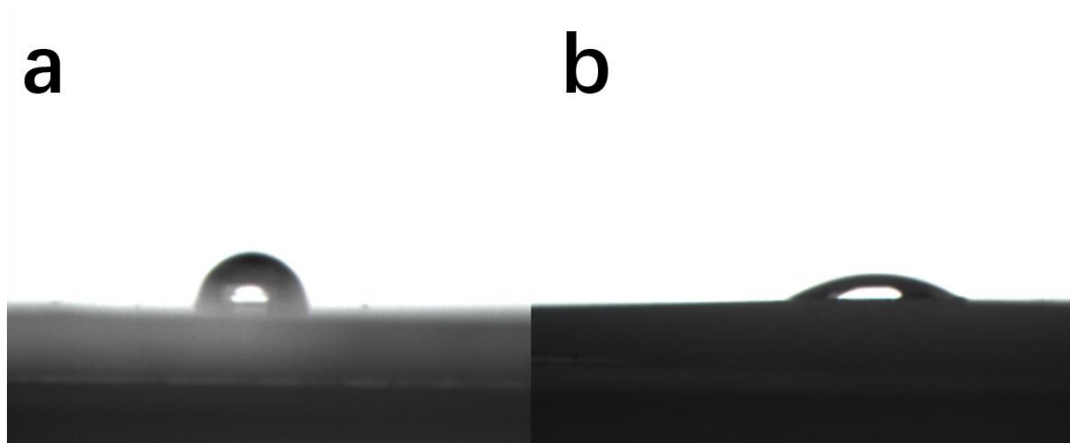


Figure S5. The WCA of PDMS coating (a) and uncoated (b) on glass substrate.

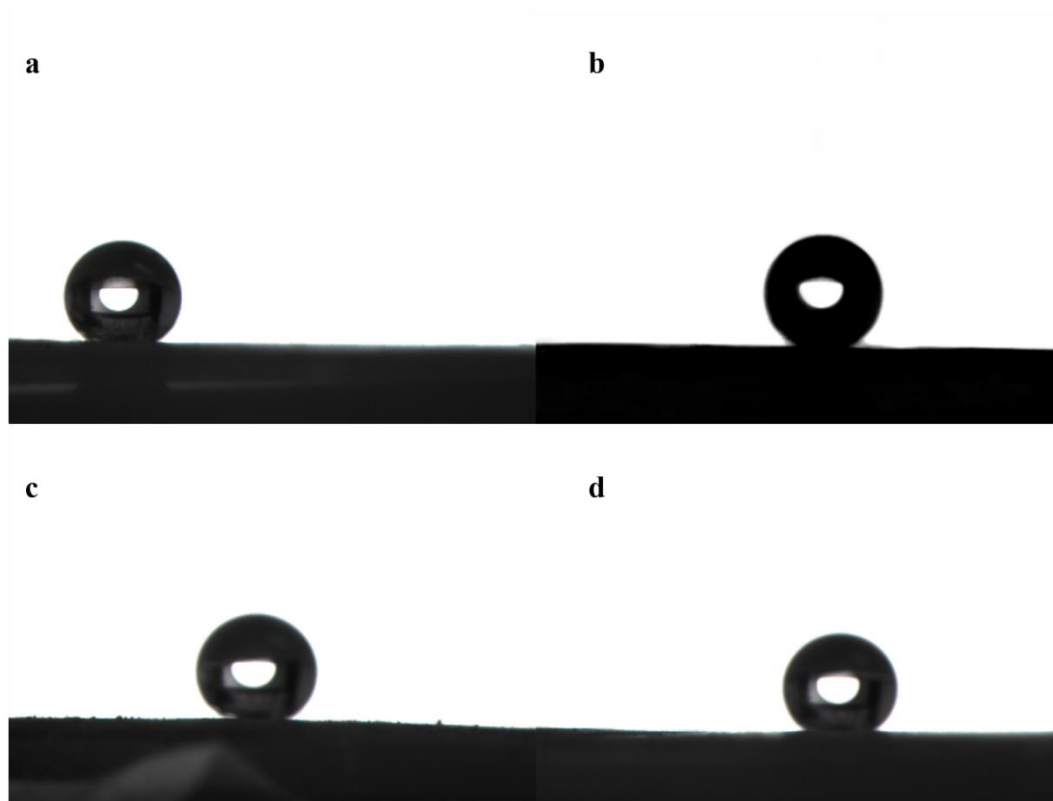


Figure S6. The WCA of the prepared mFe/ATP@Sh, heated at 200 °C for 2 h (a), kept under UV-radiation for 24 h (b), immersed in strong acid (c) and base (d) solution for 24 h.

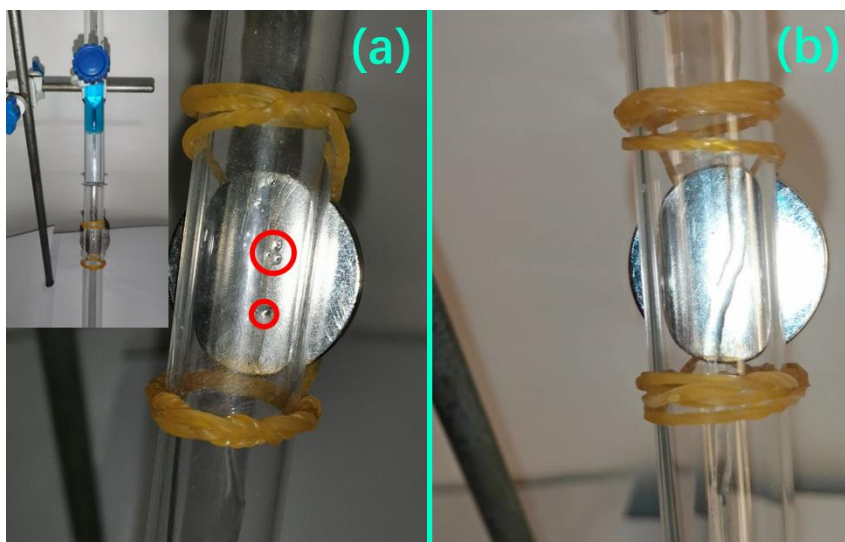


Figure S7. The stainless wire meshes (a) or the magnetic wire meshes (b) was used to fix mFe/ATP@Sh sheet after 500 cycles. The inset is the separating device that equipped with a magnet below the separate sheet. The shedding of mFe/ATP@Sh particles are marked with red circle line.

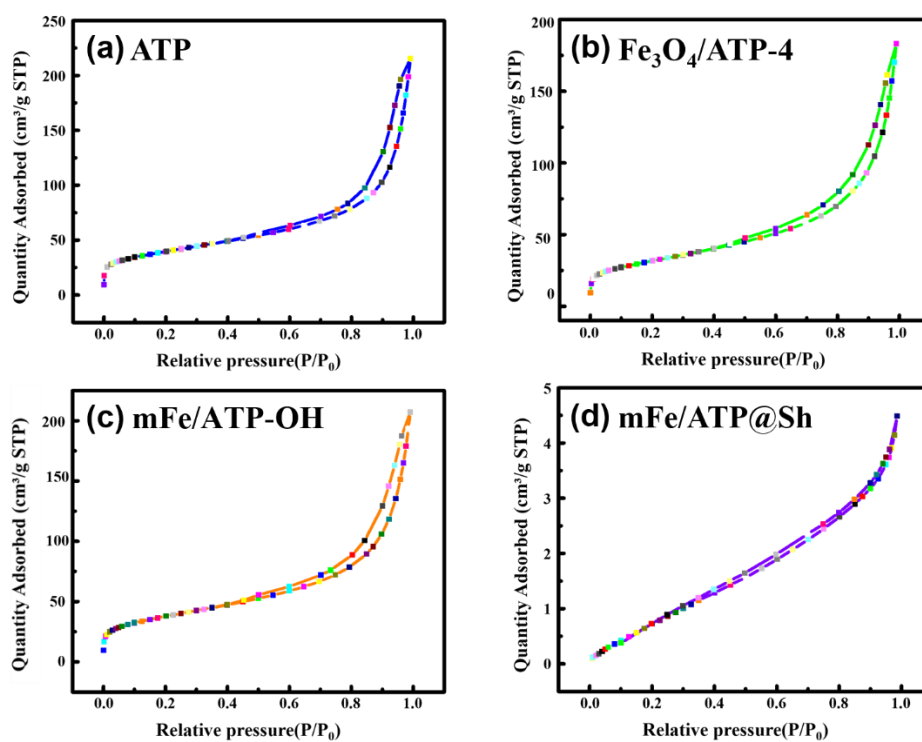


Figure S8. BJH Desorption patterns of prepared samples.

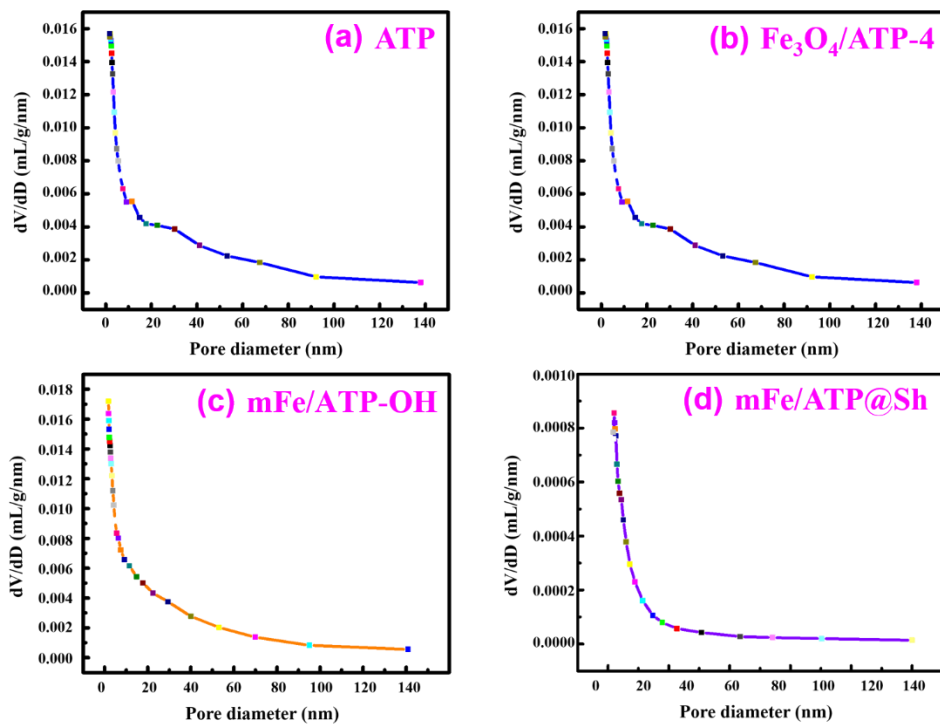


Figure S9. Pore radius of prepared samples (nm).